

## Case History

### The Geotechnical Aspects of the Haiti Earthquake

Ellen M. Rathje, University of Texas

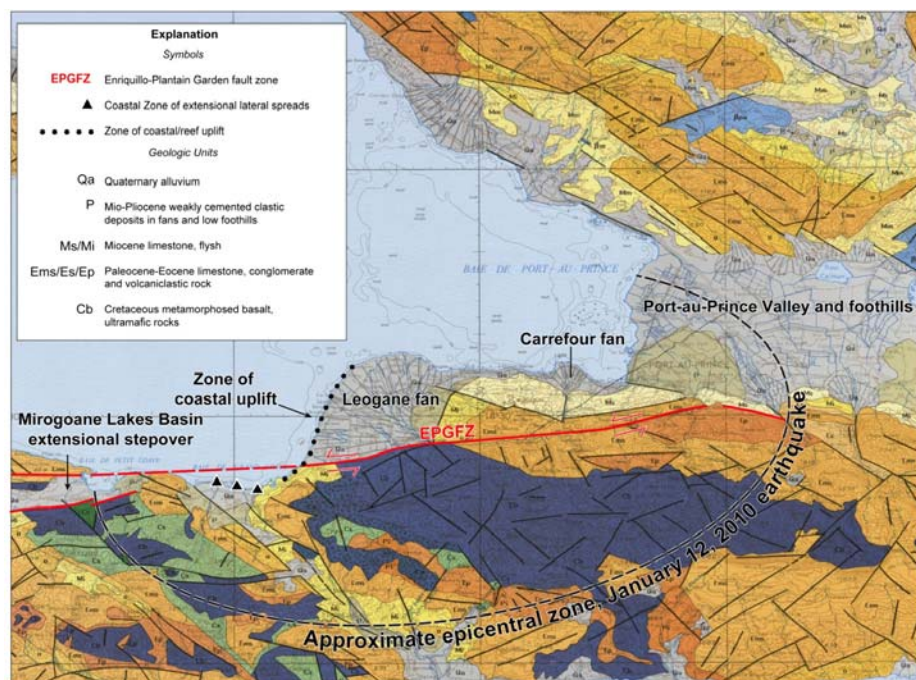
#### Introduction

On January 12, 2010 a magnitude  $M_w$  7.0 earthquake struck the Port-au-Prince region of Haiti. The Geotechnical Extreme Events Reconnaissance (GEER) Association mobilized a reconnaissance team, funded by the United States National Science Foundation, to document the geotechnical and geologic aspects of this event. The team members included: Prof. Ellen Rathje (Team leader, University of Texas), Mr. Jeff Bachhuber (Fugro/William Lettis & Associates), Prof. Brady Cox (University of Arkansas), Mr. Jim French (AMEC/Geomatrix), Prof. Russell Green (Virginia Tech), Prof. Scott Olson (University of Illinois), Prof. Glenn Rix (Georgia Tech), Mr. Oscar Suncar (University of Texas), and Mr. Donald Wells (AMEC/Geomatrix). This report is based on the extended GEER reconnaissance report by Rathje et al. (2010), which can be found at:

[http://www.geerassociation.org/GEER\\_Post%20EQ%20Reports/Haiti\\_2010/Cover\\_Haiti10.html](http://www.geerassociation.org/GEER_Post%20EQ%20Reports/Haiti_2010/Cover_Haiti10.html)

#### Seismological Aspects and Regional Geology

The  $M_w = 7.0$  Haiti earthquake occurred at 4:53 PM local time on January 12, 2010. The USGS reports that the earthquake epicenter was located at 18.457N, 72.533W, approximately 25 km west of the city of Port-au-Prince. The earthquake was initially presumed to have occurred on the Enriquillo-Plantain Garden Fault Zone (EPGFZ), a left-lateral, strike-slip fault that slips approximately 7 mm/yr (Figure 1). Although the EPGFZ is a strike-slip fault, the focal mechanism for this earthquake was identified as left-lateral/oblique. Additionally, the EPGFZ did not rupture at the surface and significant uplift occurred north of the EPGFZ (see Section 4.0, Rathje et al. 2010), such that there is significant uncertainty regarding the causative fault for the earthquake. Large earthquakes have not occurred recently on the EPGFZ, but historical records indicate that Port-au-Prince was destroyed by earthquakes in both 1751 and 1770. These events are believed to have occurred on the EPGFZ.



Modified from country-wide map by C.E.R.C.G. IMAGEO (Lambert, Gaudin, and Cohen, 1987).

Figure 1. Geologic map and faults in area affected by the Haiti earthquake (original map by Lambert, 1987)

## Case History (Continued)

### The Geotechnical Aspects of the Haiti Earthquake

The preliminary locations for aftershocks located by the regional seismic data are shown in Figure 2, along with the slip inversion derived by Caltech ([http://tectonics.caltech.edu/slip\\_history/2010\\_haiti/](http://tectonics.caltech.edu/slip_history/2010_haiti/)). The aftershocks extend over a distance of about 50 to 60 km, predominantly westward from the epicenter, and generally scattered along the trace of the EPGFZ. There is a distinct clustering of aftershocks about 30 km west of the epicenter (near Petit Goave), which corresponds with the end of the fault rupture inferred from the slip inversion as well as an extensional stepover in the fault. This extensional stepover is a natural segmentation point for the fault, and together with the other data shown in Figure 2, appears to have arrested the westward progressing fault rupture. Therefore, it appears that the major portion of the mainshock rupture process was only about 30 km long. This is somewhat shorter than would be expected for M 7 earthquake as estimated from empirical relationships (e.g., Hanks and Bakun 2008, Wells and Coppersmith 1994) that predict a rupture length of about 50 km for a M 7 earthquake. However, comparisons of rupture lengths estimated from the earthquake rupture process versus the distribution of aftershocks are not generally reliable or definitive.

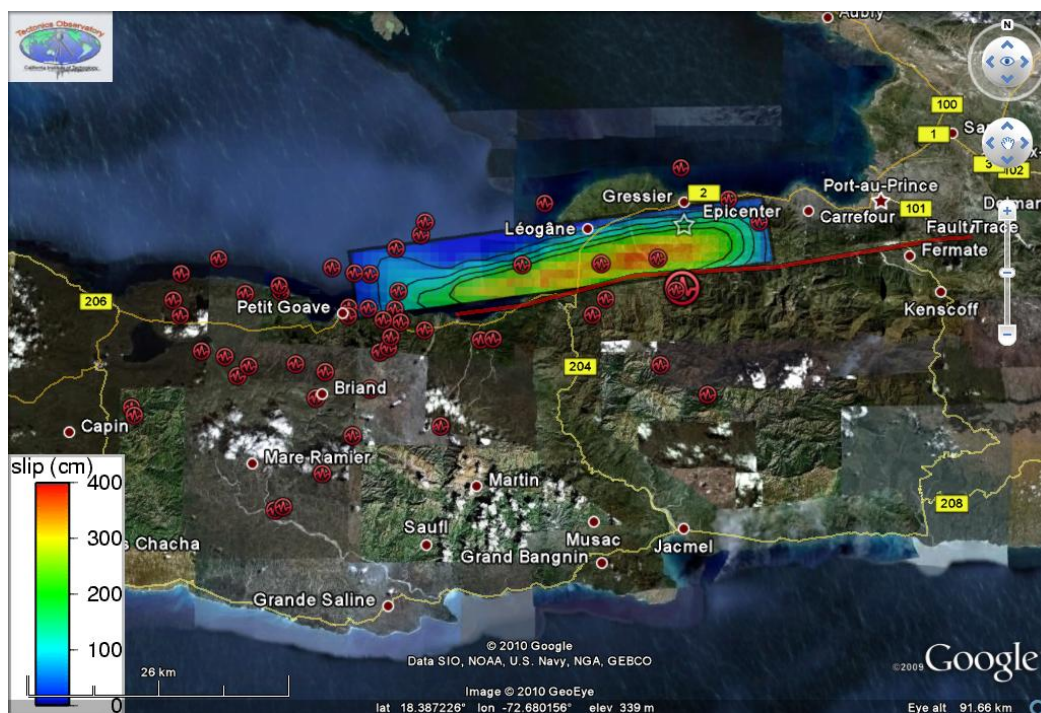


Figure 2 Aftershock distribution for the 2010 Haiti earthquake through 21 January 2010 (from USGS), along with slip inversion by Caltech ([http://tectonics.caltech.edu/slip\\_history/2010\\_haiti/](http://tectonics.caltech.edu/slip_history/2010_haiti/))

## Case History (Continued)

### The Geotechnical Aspects of the Haiti Earthquake

The earthquake-affected region is a physiographically diverse area that has undergone a complex geologic history of intrusion, tectonism, erosion, and sedimentation. The topography within the study area is relatively rugged, with steep mountain ranges and hillfronts, deeply incised streams and narrow intermountain stream valleys, and broad coastal delta fans and valleys. Figure 1 is a geologic map of the earthquake epicentral area, based on original mapping by C.E.R.C.G. IMAGEO (Lambert, Gaudin, and Cohen, 1987). The map shows the central mountainous core of the southern peninsula to be locally underlain by metamorphosed Cretaceous basalt/mafic volcanic basement, and Cretaceous-Eocene limestone, conglomerate, and clastic sedimentary rocks. An east-west trending band of Miocene and Mio-Pliocene sedimentary rock (including flysch, siltstone, shale, sandstone) occurs along the coast and southern margin of the Port-au-Prince alluvial valley.

Quaternary deposits in the earthquake-affected region include: (a) Holocene to late Pleistocene fluvial alluvium deposited in the Port-au-Prince valley and interior incised river valleys, (b) alluvial fan and colluvial wedge deposits along the margins of larger valleys, (c) coastal delta fan complexes where larger streams (e.g., Momance and Forse Rivers) discharge into the sea along the coast, and (d) artificial fill along much of the coastline within the city of Port-au-Prince. The central area of Port-au-Prince which was devastated by the earthquake spans from the relatively level floor of a large alluvial valley, southward onto low hills underlain by Mio-Pliocene deposits. Portions of the city are underlain by thick sequences of Holocene to Pleistocene alluvium in a broad downwarped basin, but zones of high damage extend onto the Mio-Pliocene bedrock. The cities of Leogane and Carrefour (Figure 1) are located on large delta fans, and are underlain by a thick sequence of Holocene to Pleistocene alluvium.

#### Damage Patterns

Earthquake-induced damage in Port-au-Prince was devastating and widespread. Yet, there were clearly areas of the city where little to no damage occurred, and areas of the city where an overwhelming majority of the buildings were severely damaged or destroyed. This section investigates, on a limited scale, some of the damage patterns around Port-au-Prince relative to geologic and topographic conditions. The damage patterns are based on a comprehensive building damage assessment performed using satellite and aerial imagery by UNOSAT (United Nations Operational Satellite Applications Programme; <http://unosat.web.cern.ch/unosat/>). The UNOSAT damage assessment in Port-au-Prince was a significant effort whereby over 90,000 buildings were visually surveyed via post-earthquake satellite and aerial imagery in order to group each structure into one of four categories: (1) Destroyed, (2) Severe Damage, (3) Moderate Damage, and (4) No Visible Damage.

Figure 3 is a shaded relief map for a portion of Port-au-Prince derived from a 1-m LIDAR DEM collected by RIT for the Worldbank (<http://ipler.cis.rit.edu/projects/haiti>). Also shown in this figure are the geologic boundaries from a geo-referenced version of the geologic map shown in Figure 1. Interestingly, the geologic map indicates that the Pliocene deposits extend almost to the coastline within the central part of the city, yet the topographic data indicate that the flat plain (which presumably corresponds to the Quaternary deposits) extends a significant distance inland. Additional geologic field mapping by the GEER team confirmed that this flat plain was underlain by Holocene and Pleistocene alluvium, and these observations were supplemented with shear wave velocity profiles measured by MASW (Cox, personal communication).

An updated geologic map of Port-au-Prince is shown in Figure 4 along with the damage data from the UNOSAT assessment. The geologic units in Figure 4 represent artificial fill (Af), Holocene alluvium (Qham) and Pleistocene fan deposits (Qpf) in the flatter areas, with Pliocene fan (Pf), Mio-Pliocene conglomerate (Mpb), and Miocene limestone (Lmst) found in the hillsides. The damaged buildings (which represent damage categories 1 through 3) are shown in red, while the undamaged buildings are shown in black.

## Case History (Continued)

### The Geotechnical Aspects of the Haiti Earthquake

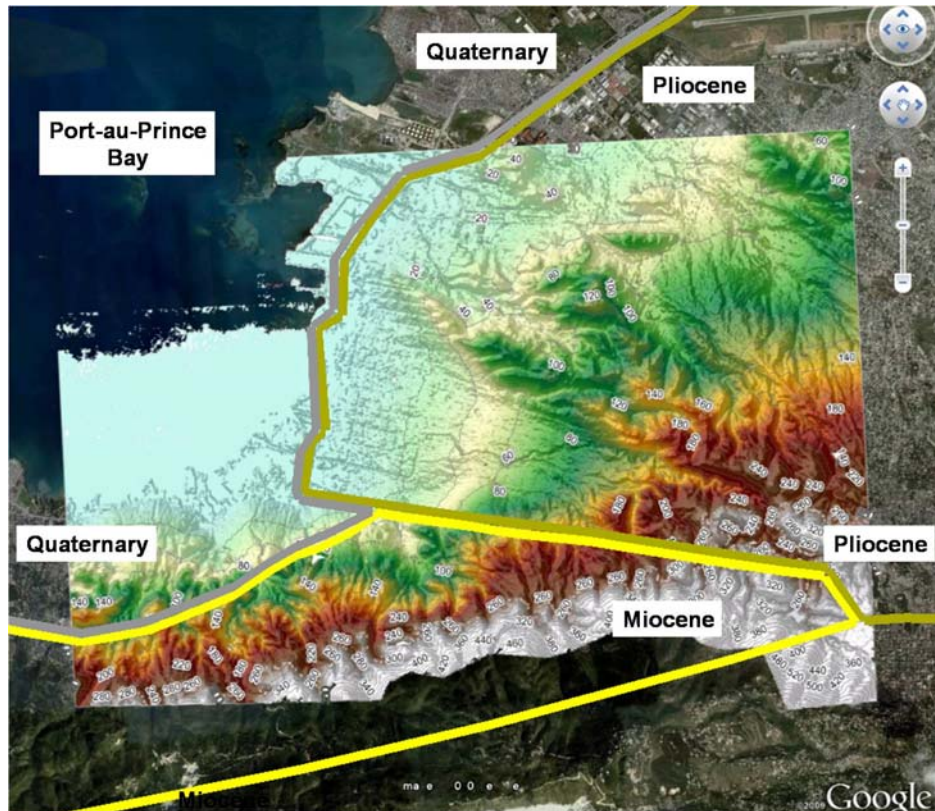


Figure 3 Shaded topographic relief map of the Port-au-Prince area with geologic boundaries from the geologic map shown in Figure 1.

In the flat, Quaternary units that underlie much of downtown Port-au-Prince, it is clear that the damage was more severe in the Holocene alluvium (Qham) than in either the artificial fill (Af) or Pleistocene fan deposits (Qpf). The percentage of buildings damaged (i.e., Damage Intensity) in the Qham deposit was approximately 38%, while the percentage of buildings damaged in the Af and Qpf deposits was approximately 10% to 15%. The concentration of damage in the Qham deposit was influenced by a combination of two factors: site amplification due to lower velocity materials ( $V_{s30} \sim 330$  m/s) and a high concentration of poorly reinforced, 2 to 5-story reinforced concrete buildings. While the Af deposits consist of lower velocity materials ( $V_{s30} \sim 250$  m/s), the Damage Intensity was smaller because they building stock in this area consisted mostly of single-story, reinforced concrete or corrugated metal structures that were less vulnerable to soft soil amplification. The Damage Intensity in the Qpf deposits was smaller due to the higher velocity materials ( $V_{s30} \sim 485$  m/s).

## Case History (Continued)

### The Geotechnical Aspects of the Haiti Earthquake

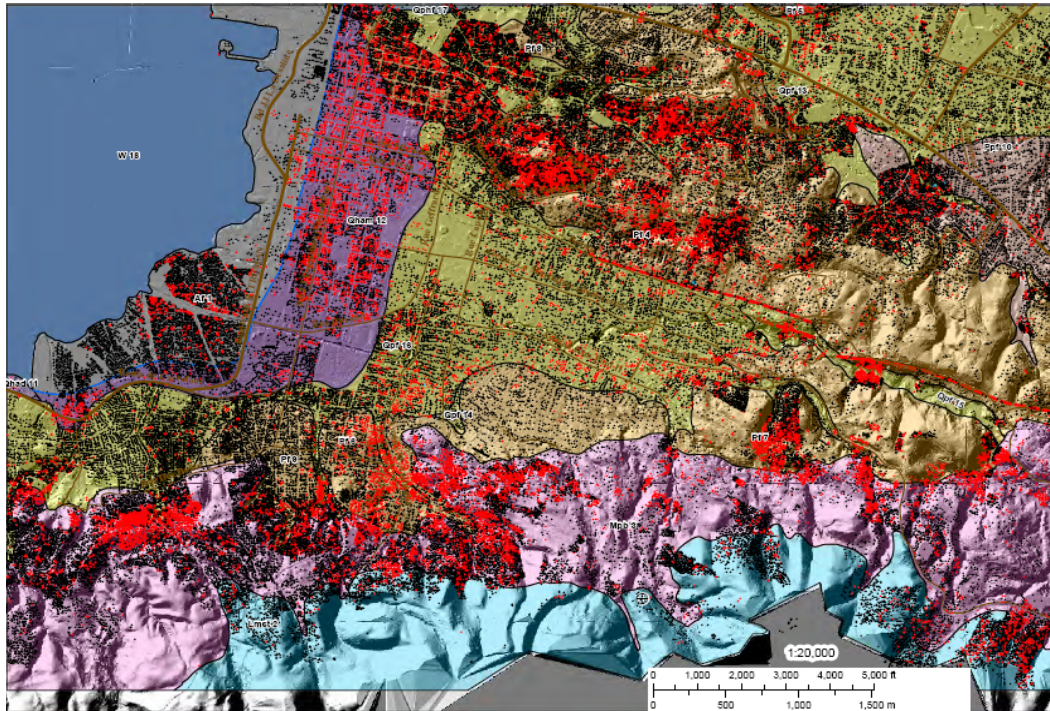


Figure 4 Revised geologic map of Port-au-Prince along with damaged buildings from UNOSAT survey (red=damaged building, black=undamaged building).

Figure 4 also shows localized areas of heavy damage in the hillsides north and south of the main alluvial plain. Damage Intensities in these zones were as large as 40 to 60%. These areas are underlain by the older Pf and Mpb deposits that consist of stiffer materials ( $V_{s30} \sim 500$  to  $550$  m/s). The slopes in Pf deposits range from  $5$  to  $20^\circ$ , while the slopes in the Mpb deposits range from  $10$  to  $40^\circ$ . These areas represent zones where it is believed that topographic amplification caused enhanced ground shaking and larger damage intensities.

#### Port Facilities and Coastal Infrastructure

The main port in Port-au-Prince is located slightly north of downtown (Figure 5) and approximately 20 to 25 km from the fault rupture. The port consists of two separate facilities built in the late 1970's and designated as the North Wharf and South Pier. The entire facility was constructed using dredged, calcareous, hydraulic fill for the staging areas, and both the North Wharf and South Pier were pile-supported.

Pre- and post-earthquake aerial images of the port are shown in Figure 6, and these images clearly show evidence of liquefaction and lateral spreading, failure of the North Wharf, and collapse of portions of the South Pier. This damage inhibited the delivery of relief supplies to areas affected by the earthquake. Light-colored areas on the ground surface in the post-earthquake image in Figure 6 are sand boils/ejecta and can be seen in the eastern half of the container storage yard and behind and between the two warehouses. Locations of large lateral spreading fissures were observed all along the shoreline.

## Case History (Continued)

### The Geotechnical Aspects of the Haiti Earthquake



Figure 5 Location of main port in Port-au-Prince.

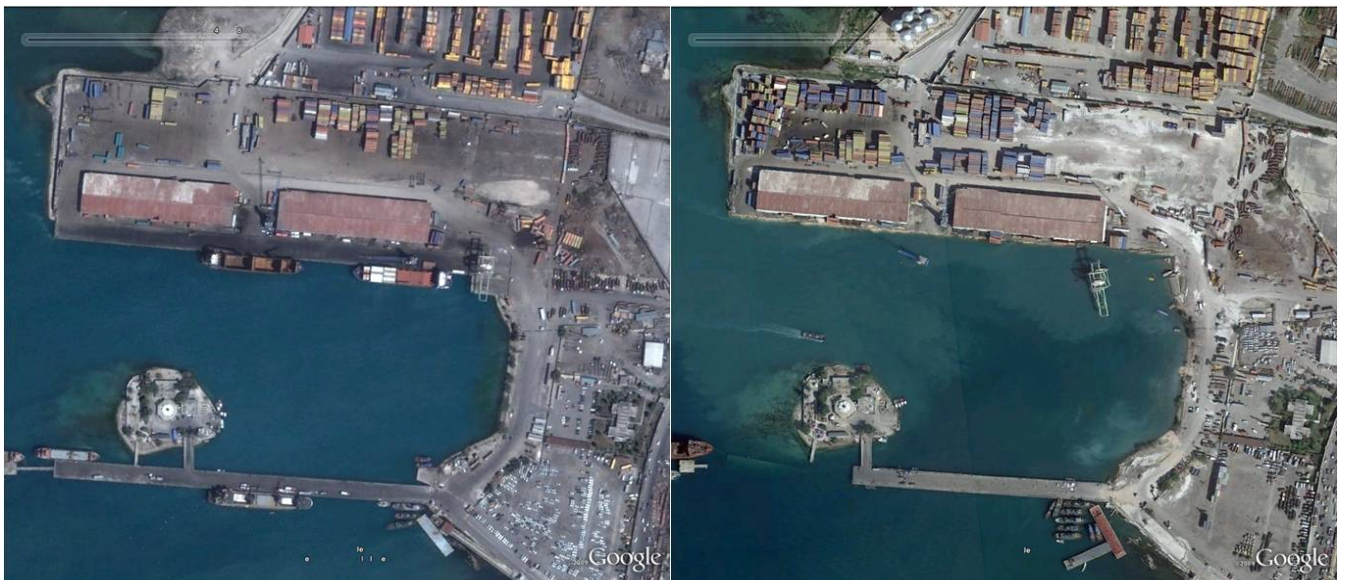


Figure 6 Pre- and post-earthquake satellite/aerial imagery (left and right, respectively) of the port at Port-au-Prince, Haiti (N18.555058°, W72.351144°). Imagery courtesy of Google Earth.

## Case History (Continued)

### The Geotechnical Aspects of the Haiti Earthquake

The North Wharf consisted of a pile-supported marginal wharf that was approximately 450 m in length and 20 m in width. The water depth is 8 to 10 m. Immediately adjacent to the wharf are two steel-frame warehouses, each approximately 150 m by 40 m. The North Wharf collapsed, most likely due to liquefaction-induced lateral spreading and the associated failure of the piles supporting the wharf. Numerous surface manifestations of liquefaction and lateral spreading were present in the vicinity of the North Wharf (e.g., Figure 7).

The warehouses along the North Wharf suffered severe damage as a result of the lateral spreading and settlement (Figure 8). Lateral spreading cracks running in the East-West direction cut through each warehouse foundation wall (Figure 8). A detailed field survey was performed of the relative elevations and lateral movements of the west warehouse slab. Due to lateral spreading, the south wall (adjacent to the shoreline) moved approximately 0.7 to 1.4 m laterally towards the shoreline. The relative elevations across the interior were variable, with the some areas almost 1 m lower than others. It appeared that the warehouses were founded on strip footings around their perimeters, which settled significantly. Settlements measured at the inland corners of the warehouses indicate 15 cm of settlement relative to the ground surface for the west warehouse and 40 cm of settlement for the east warehouse.



Figure 7 Lateral spread cracking and deformations along the North Wharf of the port.

## Case History (Continued)

### The Geotechnical Aspects of the Haiti Earthquake

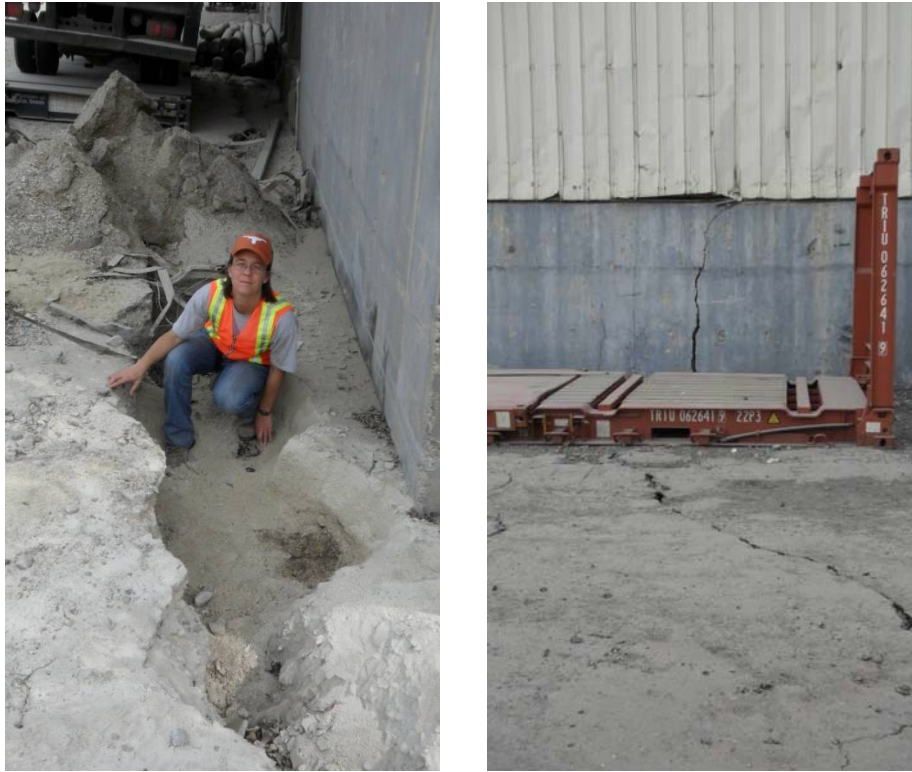


Figure 8 Ejecta and cracking adjacent to warehouses along the North Wharf

The South Pier (Figure 6) is a pile-supported structure that was originally 380 m in length and 18 m in width. A large bridge and a small pedestrian bridge that are approximately perpendicular to the longitudinal axis of the pier connected the pier to an island where the port security office is located. The western end of the pier was also connected to three dolphins by small pedestrian bridges. All of the bridges were also pile-supported structures. The piles supporting the pier are approximately 51-cm square concrete piles on 4.3 to 4.9-m centers and include both vertical and battered piles. The pile bents are 1.5 m deep and 0.9 m wide and the deck is 45 cm thick (Brian Crowder, personal communication). During the earthquake, the western-most 120 m of the South Pier and portions of the pedestrian bridges linking the dolphins collapsed and became submerged. The portion of the pier that is still standing was heavily damaged. US Army divers inspected the piles following the earthquake to determine whether the pier could support loads imposed by trucks carrying relief supplies. They found that approximately 40% of the piles were broken, 45% were moderately damaged, and 15% were slightly damaged. Generally, the batter piles were more heavily damaged than the vertical piles. The damage to the piles supporting the small pedestrian bridge connecting the South Pier to the island could be readily observed (Figure 9).

## Case History (Continued)

### The Geotechnical Aspects of the Haiti Earthquake



Figure 9 Damage to piles supporting the pedestrian bridge connecting the South Pier to the island

#### Liquefaction

Numerous liquefaction features near the coastline were identified using aerial imagery, as shown in Figure 10. Potential liquefaction-induced failures were identified up to 38 km from the epicenter and up to 26 km from the fault trace. These data plot well within the boundaries for most distal liquefaction sites proposed by Ambraseys (1988) using worldwide data (Figure 11). This suggests that the natural coastal and alluvial soils near Port-au-Prince Bay are only moderately susceptible to liquefaction, although liquefiable Quaternary sediments were generally noted only within short distances from the coast.

Generally, observed liquefaction-induced failures occurred either in fill soils placed to reclaim land for urban areas (e.g., Port-au-Prince port) or in Holocene-active delta fan lobes in coastal areas near the mouths of streams emptying into Port-au-Prince Bay. The most susceptible deposits and largest lateral spreads occurred within active Holocene delta fan lobes immediately west of the fault rupture where well-defined deltas exist where local streams discharge from a mountain front near the coast. The short distance between the mountain front and coast has not allowed significant sorting and grain size reduction in the delta lobes, such that the sediments consist predominantly layers of coarse to fine, sand and silty sand. Further inland, liquefaction features were limited to the floodplains of lower-gradient, meandering streams occasionally found north and east of Port au Prince. Most of the streams along the southern rim of Port au Prince Bay are high-gradient, braided ephemeral streams that carry coarser sediment loads. Almost no liquefaction features were identified along these streams inland of the coastline. In the city of Port au Prince, most of the streams are rather shallow and ephemeral, and have been channelized and often lined with stones or concrete. As a result, liquefaction was unlikely to occur in these drainage channels.

## Case History (Continued)

### The Geotechnical Aspects of the Haiti Earthquake



Figure 10 Liquefaction, lateral spreading, and coastal failure sites identified from post-earthquake aerial photography (sites identified as open hexagons)

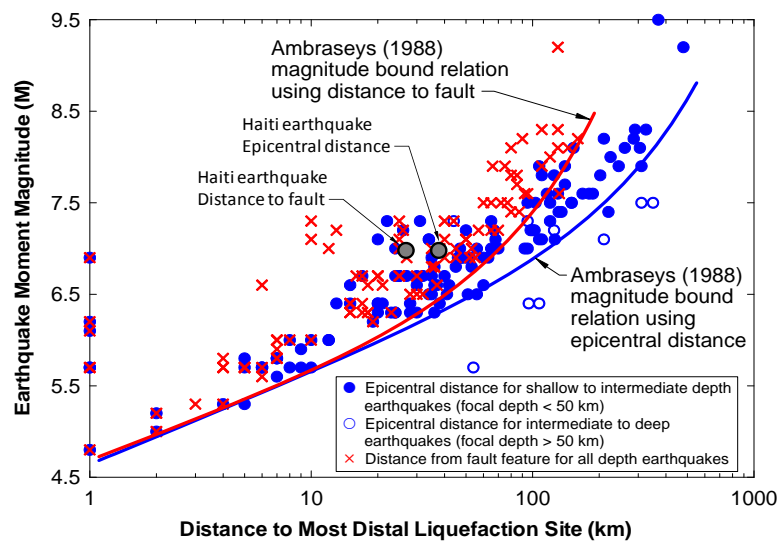


Figure 11. Comparison of most distal liquefaction sites identified in Haiti from aerial photography with worldwide data collected by Ambraseys (1988)

## Case History (Continued)

### The Geotechnical Aspects of the Haiti Earthquake

During the reconnaissance mission, the GEER team performed more detailed investigations of five potential liquefaction sites, including the Port-au-Prince port (previously discussed) and four coastal sites. One of these significant liquefaction failures occurred near the village of Fouche, close to the western edge of the fault rupture. At this site, approximately 330 m of coastline failed, as illustrated in pre- and post-earthquake imagery in Figure 12. At this site, as much as 100 m of land (perpendicular to the coast) was lost as a result of the failure. The primary manifestations of failure included scarps, cracking, and graben formation in an arcuate path along the coastline (Figure 13), as well as substantial damage to a stone wall running perpendicular to the coast and parallel to a braided stream that emptied into the bay and moderate-sized sand blows along the inland extent of the failure. One sand blow area included gravel clasts of up to about 2.5 cm in maximum dimension. The gravels may have been plucked from the sidewalls of the liquefaction feeder dike/fissure, or could have been entrained in the actual liquefied sediments.

During the reconnaissance efforts, the team conducted one Dynamic Cone Penetrometer (DCPT) test and one SASW line near several sand blows at the eastern end of the failed zone. Figure 14 presents the results of the DCPT and SASW in the failed zone. As illustrated in Figure 14, loose sand was encountered at a depth of about 0.7 m (2.5 ft), underlying a low permeability cap layer consisting of clayey sand and silty clay. The sands became medium-dense to dense at a depth of about 1.6 m (5.5 ft). The SASW shear wave velocity profile shows  $V_s \sim 120$  m/s material in the top 1 to 2 m, underlain by stiffer, non-liquefiable material ( $V_s \sim 240$  m/s).

Based on the arcuate scarp, graben formation, sand blow development, and the results of the in-situ tests, this failure is attributed to liquefaction and lateral spreading of the loose to medium dense sands below a depth of 0.7 m (2.5 ft). Headscarps and slump block scarps were up to 1.5 m high in the central parts of the failure, suggesting that failure extends perhaps 1.5 to 2 m below the original ground surface. Liquefaction likely extended to a depth of 1.6 m and may have occurred at greater depth, but penetration with the DCPT was limited in these denser sands. This failure appears to coincide directly with the presence of the braided stream dumping loose sand into the sea, rather than in the marine sands present along the coast.

#### References

- Ambraseys, N.N. (1988) "Engineering seismology, » Earthquake Engineering and Structural Dynamics, 17, 1-105.
- Hanks, T.C. and Bakun, W.H. (2008) "M-logA Observations for Recent Large Earthquakes," Bull. Seism. Soc. Am. 98, 490 - 494.
- Lambert, M., Gaudin, J. and Cohen, R. (1987) "Geologic Map of Haiti. South-East Region: Port-au-Prince," Centre d'Etudes et de Realisations Cartographiques Geographiques (CERCG), National Center for Scientific Research (CNRS), Paris, France.
- Wells, D. L., and Coppersmith, K.J. (1994) "New empirical relationships among magnitude, rupture length, rupture width, rupture area, and surface displacement" Bull. Seism. Soc. Am. 84, 974-1002.

## Case History (Continued)

### The Geotechnical Aspects of the Haiti Earthquake



Figure 12 Pre- and post-earthquake images of coastline near village of Fouche. Note in the lower, post-earthquake image the significant loss of coast as outlined in blue.

## Case History (Continued)

### The Geotechnical Aspects of the Haiti Earthquake



Figure 13 Scarp of coastal landslide near village of Fouche.

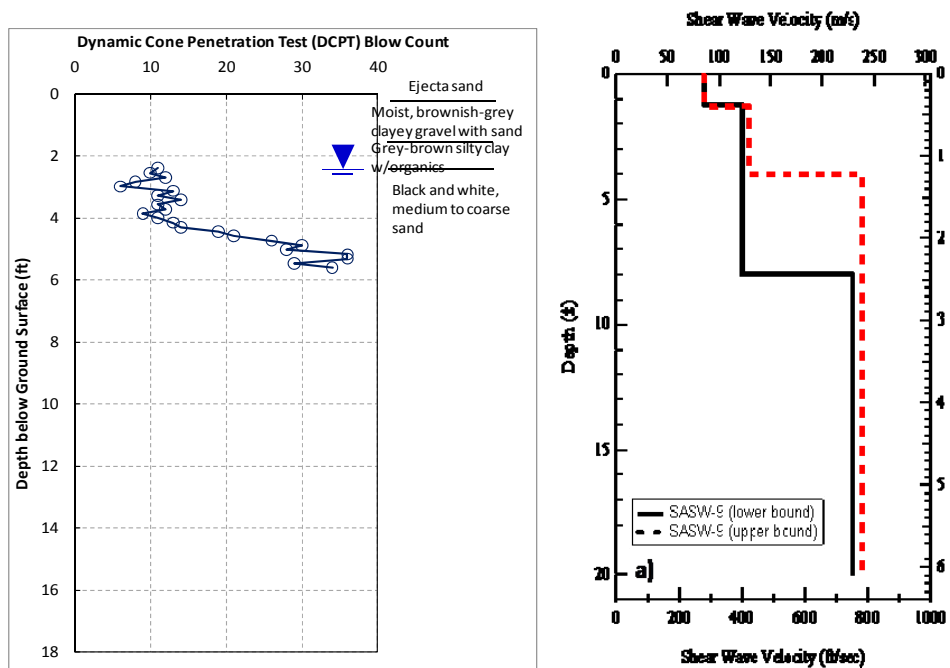


Figure 14 Results of DCPT and SASW testing at coastal failure site near village of Fouche.